Proceedings 10th NUMGE 2023
10th European Conference on Numerical Methods in Geotechnical Engineering
Zdravkovic L, Kontoe S, Taborda DMG, Tsiampousi A (eds)

https://doi.org/10.53243/NUMGE2023-249

N-PFEM modelling of plate anchor movement in sand

Y. Zhang[1], X. Zhang[1]

[1]*Department of Civil Engineering and Industrial Design, University of Liverpool, Liverpool, UK*

ABSTRACT: In this paper, we utilise a novel numerical approach, the nodal integration-based particle finite element method (N-PFEM), to investigate the horizontal movement of a vertically placed plate anchor in sands. The N-PFEM is an improved version of the particle finite element method (PFEM) for modelling large deformation problems with severe free-surface evolution. By adopting the nodal integration scheme and the generalised Hellinger-Reissner variational principle, the N-PFEM does not require variable mapping when handling history-dependent materials nor stress regularisation technique for dynamic problems. In this study, the Mohr-Coulomb model with strain-softening behaviour is adopted. The shear strength decreases according to the increasing deviatoric plastic strain. The simulated results, including both the resistance force and the failure mode, are presented and discussed.

Keywords: PFEM; nodal integration; granular material; large deformation; anchor

1 INTRODUCTION

In geotechnical engineering, many structures require foundation systems to provide resistance against vertical uplift or horizontal pullout forces. For example, structures such as sheet pile walls, bulkheads, bridge abutments and retaining walls may be unstable due to lateral earth pressures (Choudhary et al., 2017). As an efficient and economical solution, anchors are widely used in both onshore and offshore geotechnical engineering. Usually fixed to the structure and embedded in the ground to a sufficient depth, anchors can resist the uplift or lateral loading. After installing a plate anchor by excavating the ground to the required depth, the soil needs to be backfilled (Merifield et al., 2006). It is important to evaluate the the bearing capacity of the anchor in the primary design index since, improper evaluation may lead to structure failure.

The traditional finite element method (FEM), one of the most popular numerical methods, cannot handle geotechnical problems with very large deformations due to mesh distortion and severe free-surface evolution. The particle finite element method (PFEM) was proposed to overcome these issues in large deformation problems (Idelsohn et al., 2004; Idelsohn et al., 2006). The PFEM is a combination of the traditional Lagrangian FEM, the domain identification technique and the remeshing technique with mesh nodes treated as free particles after each incremental FE analysis.

However, one shortcoming of the classical PFEM is the requirement of variable mapping when considering history-dependent materials. The reason is that the remeshing operation changes the mesh topology and sequentially the quadrature points so that the variables need to be transformed from old to new quadrature points. To overcome this issue, the Smoothed PFEM (SPFEM) was proposed, which has smoothed strain estimated based on the surrounding meshes. Nodal integration is carried out so that the stress is also calculated and stored at nodes in the SPFEM (Zhang et al., 2018). Although avoiding the variables remapping is a signficant advantage of the SPFEM, the temporal instability issue arises when the smoothing technique is adopted in the conventional displacement finite element framework. In the SPFEM, the stress oscillates significantly when simulating dynamic problems so that *ad-hoc* stabilisation techniques are needed to stabilise stress fields, which complicates the implementation (Jin et al., 2021; Shafee et al., 2022).

The nodal integration based PFEM (N-PFEM) developed in (Meng et al., 2021; Zhang et al., 2022) employs the basic idea of the classical PFEM but solves a finite element formulation underpinned by the generalized Hellinger-Reissner variational principle (Zhang et al., 2019) with a nodal integration scheme This developed N-PFEM is naturally temporally stable when an implicit time integration is used, requiring no *ad-hoc* stabilisation technique. In addition, large time steps can be used to improve the efficiency of computation.

In this study, the movement of a plate anchor is investigated using the N-PFEM. This example aims to find the bearing capacity of the anchor in granular matter like sands where strain softening behaviour occurs. OPTUMG2, a finite element tool for geotechnical practitioners, is also used to verify the bearing capacity at the two limit cases: sand with peak strength and sand with residual strength. The evolution

of the reaction force as well as the failure mode in the movement of the anchor will be discussed.

2 METHODOLOGY

The N-PFEM (Meng et al., 2021; Zhang et al., 2022) used in this study was derived from a mixed variational principle, namely the generalized HR variational principle (Zhang et al., 2019). The governing equations with time discretisation are equivalent to a min-max optimisation problem, as stated in (Zhang et al., 2017; Zhang et al., 2019). The min-max problem is approximated by adopting three-node triangular elements for spatial integration over cells. The resulting maximisation problem is then reformulated as a standard second-order cone programming (SOCP) problem. In this study, the primal-dual interior point method (IPM) available in a high-performance optimisation solver MOSEK (Andersen et al., 2003; ApS, 2019) is used to solve the SOCP problem.

Figure 1 shows the construction of cells. For a domain discretised using three-node triangles (Figure 1(a)), the centroid of each triangle is connected to the mid-edge point to divide the triangle into three quadrilaterals with the same area (Figure 1(b)). Thereafter, the cell is the sum of one-third of all the triangles adjacent to each node.

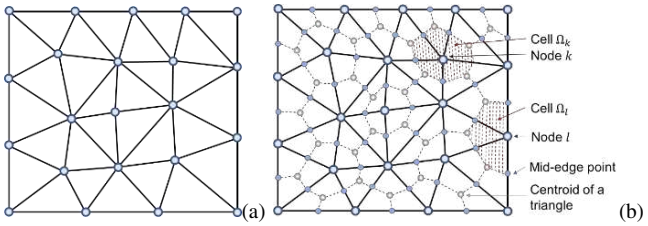

Figure 1. Construction of cells: (a) a domain; and (b) discretization using three-node triangles

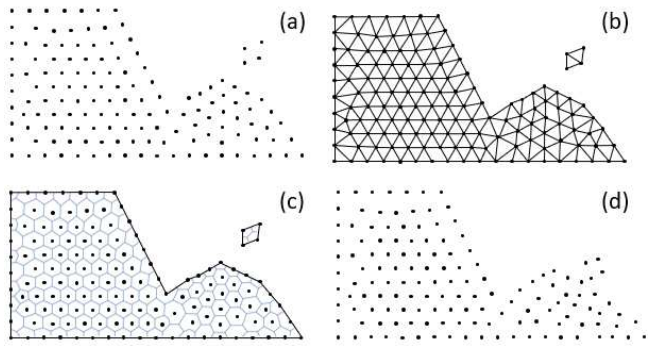

Figure 2. Computational cycles of the N-PFEM: (a) a cloud of particles; (b) triangular meshes of physical domain; (c) node-based cells; and (d) particles at the next step.

The computational cycle of the N-PFEM is similar to that of the PFEM, except that no variable mapping is required in the N-PFEM. The procedure of the N-PFEM is as follows:

(i) Use a cloud of particles to represent the computational domain at time t_n (Figure 2(a));

(ii) Use the alpha-shape method to identify the boundary of the domain and generate triangular meshes based on the particles (Figure 2(b));

(iii) Construct node-based cells according to the triangular meshes (Figure 2(c));

(iv) Solve the optimisation problem and obtain the state of filed variables, and then update the position of all particles (Figure 2(d));

(v) Repeat steps (i) to (iv) for all time steps.

3 SIMULATIONS OF PLATE ANCHOR MOVEMENT

3.1 Problem description

Figure 3 illustrates a vertically placed plate anchor that is fully buried in sand with a free surface. This plate anchor will move horizontally in response to the applied displacement u_x. The anchor has a thickness of 0.2 m and a length of 1 m. The simulation is conducted assuming a plane-strain condition, and the anchor is buried at a depth H of 3 m. The domain is discretised using 19,832 nodes and 39,202 triangular elements. The anchor is simulated to move 0.5 m in the horizontal direction. For each computational step, the applied horizontal displacement on the anchor is 0.01 m, and the time step in the simulation is 2 s to mimic a quasi-static process.

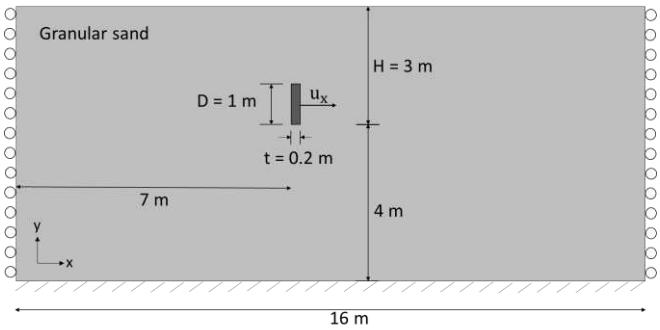

Figure 3. Geometry of the plate anchor in sand

As the anchor moves, the sand near it is disturbed resulting in a decrease in sand shear strength. This effect is reflected by a decrease in the friction angle and dilation angle. Additionally, the disturbance will also affect the density of the sand. To consider this sand softening behaviour during the movement of the anchor, the non-associated Mohr-Coulomb model with strain softening, introduced for modelling the strength loss of sand in (Yerro et al., 2016), is adopted in this study.

The parameters used to describe the softening behaviour include the friction angle ϕ, dilation angle φ, and unit weight γ. As the anchor moves, the plastic strain of the sand will increase, causing all three

parameters to decrease until they drop to their residual values. The evolution of these parameters can be evaluated by the deviatoric plastic strain ε_d^p according to the softening rules. Specifically, the evolution of the parameters is described using the following equations:

$$\phi = \phi_r + (\phi_p - \phi_r)e^{-\eta\varepsilon_d^p} \quad (1)$$

$$\varphi = \varphi_r + (\varphi_p - \varphi_r)e^{-\eta\varepsilon_d^p} \quad (2)$$

$$\gamma = \gamma_r + (\gamma_p - \gamma_r)e^{-\eta\varepsilon_d^p} \quad (3)$$

where $(\phi_p, \varphi_p, \gamma_p)$ and $(\phi_r, \varphi_r, \gamma_r)$ are the peak and residual values of the parameters, respectively. The parameter η is applied to control the softening rate (Yerro et al., 2016).

The deviatoric plastic strain invariant, ε_d^p, used in Eqs. (1)-(3) is defined as:

$$\varepsilon_d^p = \sqrt{\frac{2}{3}e_{ij}^p e_{ij}^p} \quad (4)$$

where e_{ij}^p is the deviatoric part of the plastic strain tensor.

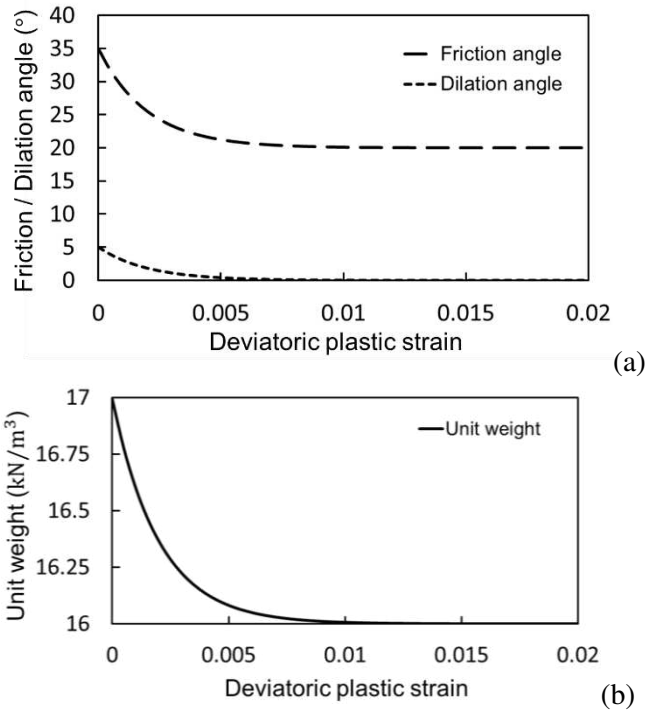

Figure 4. Evolution of soil parameters against deviator plastic strain in N-PFEM model with shape factor parameter $\eta = 500$: (a) friction and dilation angle; and (b) unit weight.

Values of the material parameters used in this study are detailed in Table 1, and the evolution of the friction angle, dilation angle and unit weight against the deviatoric plastic strain are shown in Figure 4. As illustrated, the decreasing velocity of the friction angle ϕ, dilation angle φ and unit weight γ is quite high. When the deviator plastic strain is 0.01, all the three parameters drop down to almost their residual values $(\phi_r, \varphi_r, \gamma_r)$.

Table 1. Soil parameters of the sand

Soil parameters	Value
Young's modulus (kPa)	20,000
Poisson's ratio (-)	0.33
Cohesion (kPa)	0
Shape factor parameter	500
Peak friction angle (°)	35
Residual friction angle (°)	20
Peak dilation angle (°)	5
Residual dilation angle (°)	0
Peak unit weight ($\mathbf{kN/m^3}$)	17
Residual unit weight ($\mathbf{kN/m^3}$)	16

3.2 Results

To verify the accuracy of the N-PFEM programming, two cases are simulated using the peak strength $(\phi_p, \varphi_p, \gamma_p)$ and the residual strength $(\phi_r, \varphi_r, \gamma_r)$, without updating the nodes positions and meshes. The results of the bearing capacity of these two cases are then compared with the results obtained from OPTUMG2 using the same model geometry and soil parameters. As shown in Figure 5, the two dash lines represent the final bearing capacity obtained from OPTUMG2 for sands under the peak strength condition and residual strength condition, respectively. It is clear that the maximum horizontal resistance forces exerted on the anchor from N-PFEM simulation agree with those from OPTUMG2 for both cases, although the reaction force fluctuates slightly for the case of using the peak friction angle.

The softening behaviour of the sand is then considered using Eqs. (1)-(4). As shown in Figure 5, there is a peak horizontal reaction force in the early stage of the movement when the horizontal moving distance is 0.04 m. After that, due to the accumulated plastic strain of the sand in the failure zone, the strength of the sand decreases leading to the reduction of the reaction force before it reaches a residual stable value of 185 kN between the peak and residual values. To estimate the infulance of the shape factor parameter η, the model is also simulated with $\eta = 400$ and 600, respectively (Figure 5). When the shape factor parameter η changes, the variation trend of the horizontal reaction force against the horizontal moving distance is the same. The forces will always go up firstly to a peak value when the horizontal moving distance of the anchor is between 0 to 0.1 m and then go down until the anchor moves about 0.2 m, after which the reaction force remains stable from 0.2 m to 0.5 m. Although the peak horizontal force will change, the final residual stable forces are still very similar and between the peak

and residual values when using these three different shape factor parameters.

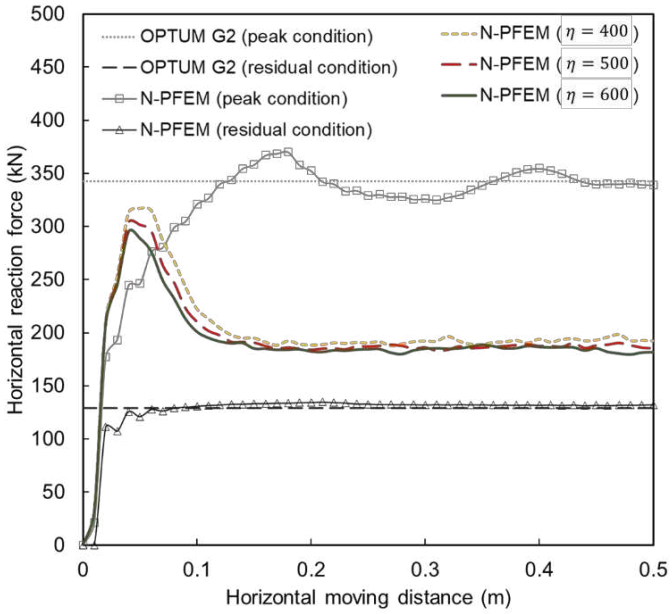

Figure 5. Changes of the horizontal reaction force against the moving distance

Figure 6 shows the distribution of the deviatoric plastic strain at the moving distance of the plate anchor being 0.1 m, 0.3 m and 0.5 m when considering the sand softening with $\eta = 500$. The maximum plastic strain shown in Figure 6 is 0.01 as all of the friction angle, dilation angle and unit weight are almost decreased to their residual values when the plastic strain is 0.01. Figure 6 shows there will be a surface failure mode in the case that the buried depth of the anchor is 3 m. With the increasing of the horizontal moving distance of the anchor, the deviatoric plastic strain of the failure zone is also increasing. The increasing deviatoric plastic strain results in the strength loss of the sand, including the decrease of the friction angle, dilation angle and unit weight. Therefore, the final bearing capacity is less than the value when using peak strength but greater than the value when using residual strength.

From a moving distance of 0.1 m (Figure 6(a)) to 0.3 m (Figure 6(b)), the width of the shear band increases, and the reaction force decreases from 210 kN to 186 kN (Figure 5). Then, from a moving distance of 0.3 m (Figure 6(b)) to 0.5 m (Figure 6(c)), the area of the old shear band does not increase significantly, and a new shear band appears inside of the old one. However, the reaction force almost remains unchanged, as shown in Figure 5. Therefore, for a buried depth of 3 m, with the horizontal moving of the anchor, a surface failure shear band will appear, and its width will increase. During this time, the horizontal force will initially increase to a peak value and then decrease until it retains a stable value. During the stable force period, although a new shear band appears inside the old failure band, the reaction force remains stable.

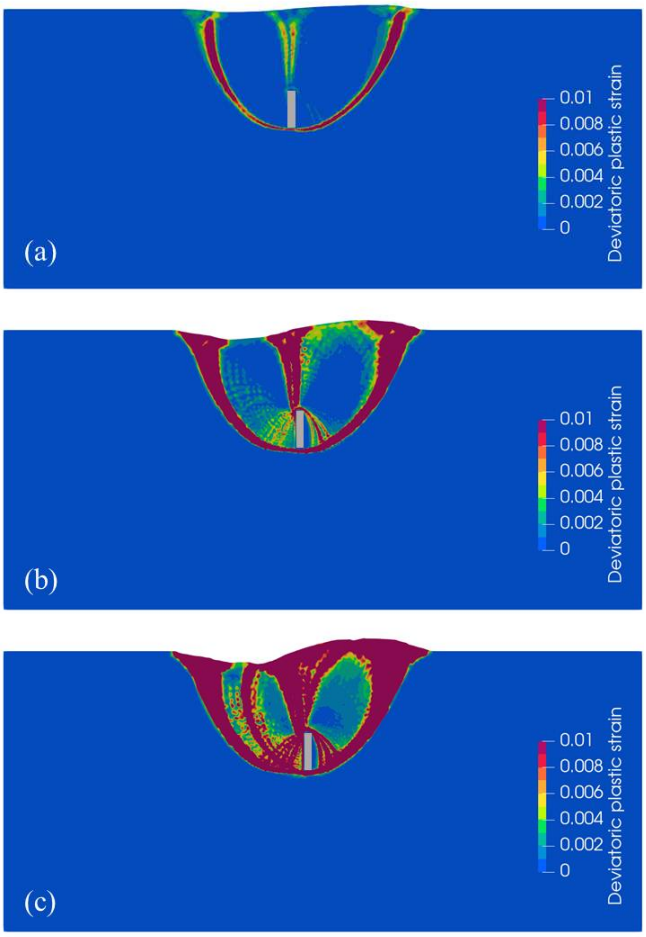

Figure 6. Schematic diagram of the mapping of the deviatoric plastic strain of the anchor movement in sand with the sand softening shape factor η=500 at: (a) horizontal moving distance is 0.1 m; (b) horizontal moving distance is 0.3 m; and (c) horizontal moving distance is 0.5 m.

4 CONCLUSIONS

The Node Integration based PFEM (N-PFEM) is an improved version of traditional PFEM, developed to simulate large deformation soil mechanics problems. Integrals of terms related to stress and strain in the N-PFEM are carried out over cells rather than finite elements, so that variable mapping is not required. In this study, the N-PFEM is used to investigate the mechanisms governing horizontal movement of a plate anchor in sand with an originally buried depth of 3 m, considering sand softening. The accuracy of the N-PFEM is confirmed through comparing results obtained from OPTUMG2 and from the N-PFEM simulations without considering sand softening, using small deformation analysis. When sand softening is considered, a small change in the shape factor parameters η (from 400 to 600) does not alter the variation trend or the final stable value of bearing capacity. The reaction force always rises to a peak value and then decreases until it reaches a stable value, and the final stable bearing capacity is as expected, between

the values in the two limit cases. Additionally, a clear shear band will appear near the anchor, forming a surface failure mode as the anchor moves. During the stable reaction force period, although a new shear band appears inside the old one, the bearing capacity remains stable.

5 ACKNOWLEDGEMENTS

This work was supported by the New Investigator Award grant of UK Engineering and Physical Sciences Research Council (EP/V012169/1) and the Royal Society International Exchanges grant (IEC/NSFC/191261).

6 REFERENCES

Andersen, E. D., et al. 2003. *On implementing a primal-dual interior-point method for conic quadratic optimization*. Mathematical Programming **95**(2): 249-277.

ApS, M. 2019. *Mosek optimization toolbox for matlab*. User's Guide and Reference Manual, Version **4**.

Choudhary, A. K., Dash S. K. 2017. *Load-carrying mechanism of vertical plate anchors in sand*. International Journal of Geomechanics **17**(5): 04016116.

Idelsohn, S. R., et al. 2006. *Fluid–structure interaction using the particle finite element method*. Computer methods in applied mechanics and engineering **195**(17-18): 2100-2123.

Idelsohn, S. R., et al. 2004. *The particle finite element method: a powerful tool to solve incompressible flows with free-surfaces and breaking waves*. International journal for numerical methods in engineering **61**(7): 964-989.

Jin, Y.-F., et al. 2021. *A stable node-based smoothed PFEM for solving geotechnical large deformation 2D problems*. Computer Methods in Applied Mechanics and Engineering **387**: 114179.

Meng, J., et al. 2021. *A nodal-integration based particle finite element method (N-PFEM) to model cliff recession*. Geomorphology **381**: 107666.

Merifield, R., Sloan S. 2006. *The ultimate pullout capacity of anchors in frictional soils*. Canadian geotechnical journal **43**(8): 852-868.

Shafee, A., Khoshghalb A. 2022. *Particle node-based smoothed point interpolation method with stress regularisation for large deformation problems in geomechanics*. Computers and Geotechnics **141**: 104494.

Yerro, A., et al. 2016. *Run-out of landslides in brittle soils*. Computers and Geotechnics **80**: 427-439.

Zhang, W., et al. 2018. *Smoothed particle finite-element method for large-deformation problems in geomechanics*. International Journal of Geomechanics **18**(4): 04018010.

Zhang, X., et al. 2022. *An implicit nodal integration based PFEM for soil flow problems*. Computers and Geotechnics **142**: 104571.

Zhang, X., et al. 2019. *A unified Lagrangian formulation for solid and fluid dynamics and its possibility for modelling submarine landslides and their consequences*. Computer Methods in Applied Mechanics and Engineering **343**: 314-338.

Zhang, X., et al. 2017. *Lagrangian modelling of large deformation induced by progressive failure of sensitive clays with elastoviscoplasticity*. International Journal for Numerical Methods in Engineering **112**(8): 963-989.